

BOOSTING UNSUPERVISED CONTRASTIVE LEARNING USING DIFFUSION-BASED DATA AUGMENTATION FROM SCRATCH

Zelin Zang^{1,2,4*}, Hao Luo^{2,3}, Kai Wang⁴, Panpan Zhang⁴, Fan Wang^{2,3}, Stan.Z Li^{1†}, Yang You⁴

¹ AI Lab, Research Center for Industries of the Future, Westlake University, China

² DAMO Academy, Alibaba Group

³ Hupan Lab, Zhejiang Province

⁴ National University of Singapore

zangzelin@westlake.edu.cn, michuan.lh@alibaba-inc.com,

{kai.wang, panpan.zhang}@comp.nus.edu.sg,

fan.w@alibaba-inc.com, Stan.Z.Li@westlake.edu.cn,

youy@comp.nus.edu.sg

ABSTRACT

Unsupervised contrastive learning methods have recently seen significant improvements, particularly through data augmentation strategies that aim to produce robust and generalizable representations. However, prevailing data augmentation methods, whether hand-crafted or based on foundation models, tend to rely heavily on prior knowledge or external data. This dependence often compromises their effectiveness and efficiency. Furthermore, the applicability of most existing data augmentation strategies is limited when transitioning to other research domains, especially science-related data. This limitation stems from the paucity of prior knowledge and labeled data available in these domains. To address these challenges, we introduce **DiffAug**-a novel and efficient **Diffusion**-based data **Augmentation** technique. DiffAug aims to ensure that the augmented and original data share a smoothed latent space, which is achieved through diffusion steps. Uniquely, unlike traditional methods, DiffAug first mines sufficient prior semantic knowledge about the neighborhood. This provides a constraint to guide the diffusion steps, eliminating the need for labels, external data/models, or prior knowledge. Designed as an architecture-agnostic framework, DiffAug provides consistent improvements. Specifically, it improves image classification and clustering accuracy by 1.6% ~ 4.5%. When applied to biological data, DiffAug improves performance by up to 10.1%, with an average improvement of 5.8%. DiffAug shows good performance in both vision and biological domains. The code will be available upon the paper’s acceptance¹.

1 INTRODUCTION

Contrastive learning, as highlighted by various studies (He et al., 2020; Chen et al., 2020; Cui et al., 2021; Wang & Qi, 2022; Assran et al., 2022; Zang et al., 2023), has become pivotal in vision (He et al., 2021; Zang et al., 2022b), natural language processing (Rethmeier & Augenstein, 2023), and biological (Yu et al., 2023; Krishnan et al., 2022). Its utility in generating positive and negative samples is particularly notable. Data augmentation, due to its straightforward yet effective approach, has found its way into several leading contrastive learning frameworks such as SimCLR (Chen et al., 2020), BYOL (Grill et al., 2020), and DLME (Zang et al., 2022b). A wealth of research (Tian et al., 2020; Zhang & Ma, 2022; Peng et al., 2022; Zhang et al., 2023) suggests that data augmentation empowers contrastive learning with robust, generalized representations, simultaneously acting as a preventative measure against model collapse.

*This work was done when Zelin Zang was intern at DAMO Academy.

†Stan.Z Li is the corresponding author of this paper.

¹<https://github.com/zangzelin/DiffAug>

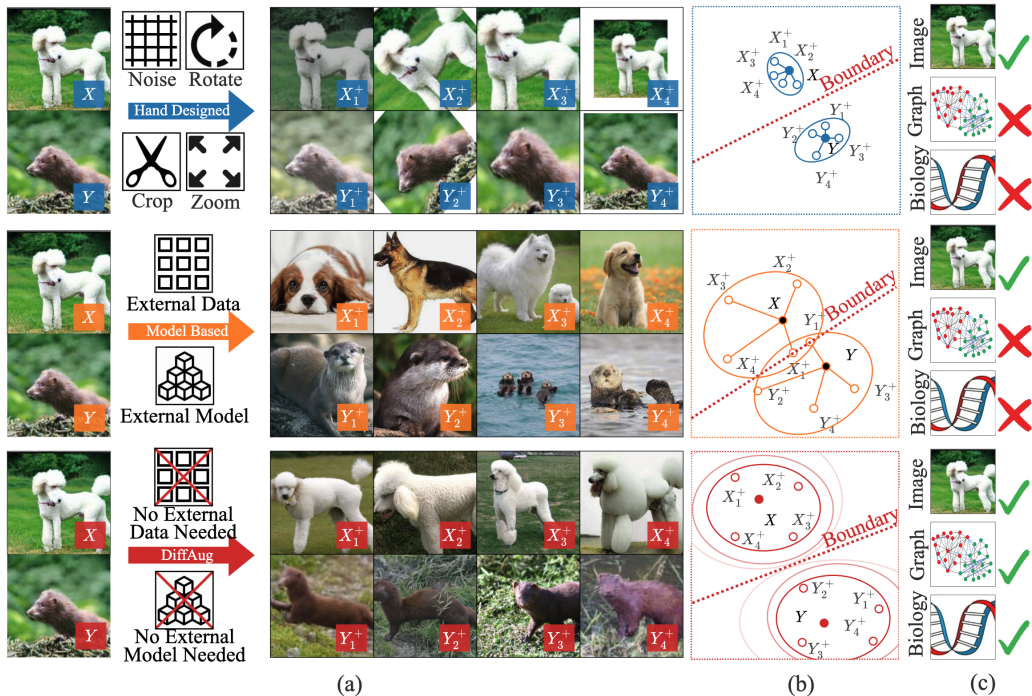


Figure 1: Overview of the proposed method. (a) The hand designed augmentation method, the vanilla augmentation method and our proposed diffusion model based augmentation method produce pictures. (b) Representation of the augmentation of the three methods in semantic space (c) The adaptability of the three methods to image data, graph data, and mRNA data.

Historically, data augmentation methodologies can be divided into two major categories: hand designed strategies and model based strategies (Xu et al., 2023). In the realm of vision, hand-crafted methods often encompass techniques like color jitter (Yan et al., 2022), rotation (Maharana et al., 2022), random cropping (Cubuk et al., 2020), and noise introduction (Khalifa et al., 2022). As depicted in Figure 1(a), these manual strategies tend to yield samples closely resembling the original image, resulting in a modest enhancement in performance (Maharana et al., 2022). In contrast, model based techniques leverage prior knowledge from labeled data and pretrained models for data generation (Huang et al., 2018; Cubuk et al., 2019; Chadebec et al., 2022; Li et al., 2021b). A potential caveat is that the augmented data’s distribution might be skewed by the labeled data and external models, leading to domain shifts (Peng et al., 2022; Zhang et al., 2023).

Furthermore, the application of the aforementioned hand designed methods to niche domains, such as gene data (Huang et al., 2022) or protein data (Li & Zhang, 2022; Sun et al., 2022), presents a challenge. The inherent complexity and lack of intuitive understanding of such data makes it cumbersome to devise effective augmentations. In these domains, simplistic approaches like perturbation (Huang et al., 2022) and random masking (Theodoris et al., 2023) are often employed. This observation sparks the question: Can a universal data augmentation strategy be formulated that transcends domain-specific expertise or the need for additional data?

To answer this, we introduce DiffAug, a versatile and controllable data augmentation paradigm rooted in diffusion processes. The hallmark of DiffAug lies in its ability to automate semantic summarization, subsequently crafting augmented data grounded in this summarization without resorting to labels or an external foundational model. Its control mechanism ensures that the semantic deviation of the created semantics can be precisely modulated via a specific model parameter. At its core, DiffAug comprises two intertwined modules: the semantic encoder and the diffusion generation. These work in tandem to facilitate unsupervised data augmentation. The semantic encoder, using a ‘soft contrastive loss’, crafts a latent representation that serves as condition vectors for the diffusion generation module. The latter, in turn, iteratively creates new augmented data in the input space, maintaining distinct monosemantic similarities based on these condition vectors and a controlled hyper-parameter.

Table 1: **Innovation in application.** The requirements and areas of applicability of the three different data augmentation methods to external information.

Aug. Methods	Need No Pretrained Models	Need No Additional Data	Need No Manual Design	Applicable to Various Fields
Hand Designed	×	✓	×	×
Model Based	×	×	✓	×
DiffAug (Ours)	✓	✓	✓	✓

When evaluated empirically, DiffAug, as an architecture-neutral framework, consistently amplifies the performance of leading algorithms like SimCLR, MoCo-V2, MAE (LT), BYOL, SimSiam, and DLME. The improvements range from 1.8% to 4.5% in classification accuracy and 1.6% to 6.0% in clustering accuracy across benchmarks like CIFAR-10, CIFAR-100, STL10, and Tiny-ImageNet. Notably, its potency is even more evident in the genes and proteins data realm. For datasets like HCL, Gast, Sam, MCA, and MAU, the performance surge reaches up to 1.1%, with an average elevation of 5.8%. To the best of our comprehension, DiffAug emerges as the pioneering universal data augmentation framework, showcasing commendable results in both the vision and biological sectors. In summary, the differences between DiffAug and other baseline methods is shown in Table 1, the main contributions of this paper are as follows:

- We develop a novel data augmentation framework, called DiffAug, which is designed to generate positive data for unsupervised contrastive learning.
- The proposed DiffAug does not require external data or hand-designed rules, and it can be applied to various model, such as vision, gene, and protein.
- The experimental results demonstrate the effectiveness of DiffAug in improving contrastive learning performance on various tasks. DiffAug open up new possibilities for generating high-quality positive data and advancing the state-of-the-art in unsupervised learning methods.

2 RELATED WORK

Generative Models Generative models have been the subject of growing interest and rapid advancement. Earlier methods, including VAEs (Kingma & Welling, 2014) and GANs (Goodfellow et al., 2014), showed initial promise generating realistic images, and were scaled up in terms of resolution and sample quality (Brock et al., 2019; Razavi et al., 2019). Despite the power of these methods, many recent successes in photorealistic image generation were the result of diffusion models (Ho et al., 2020; Nichol & Dhariwal, 2021; Saharia et al., 2022; Nichol et al., 2022; Ramesh et al., 2022). Diffusion models have been shown to generate higher-quality samples compared to their GAN counterparts (Dhariwal & Nichol, 2021), and developments like classifier free guidance (Ho & Salimans, 2022) have made text-to-image generation possible. Recent emphasis has been on training these models with internet-scale datasets like LAION-5B (Schuhmann et al., 2022). Generative models trained at internet-scale (Rombach et al., 2022; Saharia et al., 2022; Nichol et al., 2022; Ramesh et al., 2022) have unlocked several application areas where photorealistic generation is crucial.

Synthetic Image Data Generation Training neural networks on synthetic data from generative models was popularized using GANs (Antoniou et al., 2017; Tran et al., 2017; Zheng et al., 2017). Various applications for synthetic data generated from GANs have been studied, including representation learning (Jahani et al., 2022), inverse graphics (Zhang et al., 2021a), semantic segmentation (Zhang et al., 2021b), and training classifiers (Tanaka & Aranha, 2019; Dat et al., 2019; Yamaguchi et al., 2020; Besnier et al., 2020; Xiong et al., 2020; Wickramaratne & Mahmud, 2021; Haque, 2021). More recently, synthetic data from diffusion models has also been studied in a few-shot setting (He et al., 2022). These works use generative models that have likely seen images of target classes and, to the best of our knowledge, we present the first analysis for synthetic data on previously unseen concepts.

Synthetic Biology Data Generation The realm of synthetic biology has witnessed a surge in the utilization of data-driven approaches, particularly with the advent of advanced computational mod-

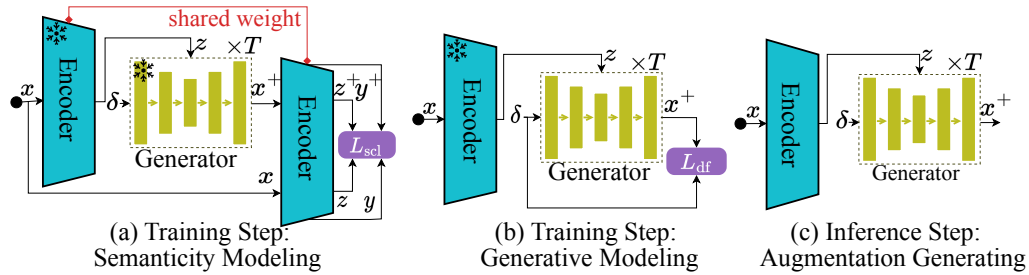


Figure 2: **The framework of DiffAug.** DiffAug includes a semantic encoder $\text{Enc}(\cdot|\theta)$ and a diffusion generator $\text{Gen}(\cdot|\phi)$. (a) and (b) is the training step of DiffAug. The (c) is the inference step which generating new augmentation data. In inference step, the $\text{Enc}(\cdot)$ maps the input data \mathbf{x} to the discriminative latent space \mathbf{z} , then the diffusion generator $\text{Gen}(\cdot)$ generates new augmentation result \mathbf{x}^+ .

els. The generation of synthetic biological data has been instrumental in predicting protein structures (McGibbon et al., 2023). The use of Generative Adversarial Networks (GANs) has also found its way into this domain, aiding in the creation of synthetic DNA sequences (Zheng et al., 2023; Li & Zhang, 2022; Han et al., 2019) and simulating cell behaviors (Botton et al., 2022). Furthermore, the integration of machine learning with synthetic biology has paved the way for innovative solutions in drug discovery (Blanco-Gonzalez et al., 2023; McGibbon et al., 2023). Unlike the synthetic image data generation, where models have often seen images of target classes, synthetic biology data generation often grapples with the challenge of generating data for entirely novel biological entities. This presents a unique set of challenges and opportunities, pushing the boundaries of what synthetic data can achieve in the realm of biology.

3 METHODS

In the context of unsupervised data augmentation, the training dataset providing potential semantic categories is denoted as $\mathcal{D}_t = \{\mathbf{x}_i\}_{i=1}^N$, where N is the size of the training set. To boost the training efficiency of unsupervised contrastive learning with positive samples generated by the diffusion model, a novel framework called DiffAug is proposed. DiffAug is based on the diffusion model and is not limited by the data domain, providing a novel solution for unsupervised data enhancement tasks.

The DiffAug framework is illustrated in Fig. 2. DiffAug consists of two main components, a semantic encoder $\text{Enc}(\cdot|\theta)$ and a diffusion generator $\text{Gen}(\cdot|\phi)$. The $\text{Enc}(\cdot|\theta)$ maps the input data \mathbf{x}_i to the discriminative latent space, and the generator $\text{Gen}(\cdot|\phi)$ generates new data with a semantic vector. The semantic encoder $\text{Enc}(\cdot|\theta)$ and the diffusion generator $\text{Gen}(\cdot|\phi)$ are jointly trained through two losses (see Fig. 2(a) and Fig. 2(b)).

In the semantic modeling stage, the semantic encoder $\text{Enc}(\cdot|\theta)$ is trained using the soft contrastive learning loss (Zang et al., 2022b). Initially, we create a background set around a central piece of data \mathbf{x}_c ,

$$\mathcal{X} = \{\mathbf{x}_c, \mathbf{x}_1, \dots, \mathbf{x}_j, \dots, \mathbf{x}_B\}, \begin{cases} \mathbf{x}_j \sim \mathcal{D}_t & \text{if } \mathcal{H}_{ij} = 0 \\ \mathbf{x}_j \sim A_{\text{ug}}(\mathbf{x}_c) & \text{if } \mathcal{H}_{ij} = 1 \end{cases} \quad (1)$$

where B is the number of background data points, the scalar indicator \mathcal{H}_{ij} , \mathbf{x}_j is neither an augmentation of \mathbf{x}_c nor sample from the different input data. The $A_{\text{ug}}(\mathbf{x}_c)$ is a data augmentation strategy, for the traditional scheme, $A_{\text{ug}}(\mathbf{x}_c)$ represents operations such as random cropping (Cubuk et al., 2020) or data mixup (Zhang et al., 2017). In this paper, $A_{\text{ug}}(\mathbf{x}_c) = \text{Gen}(\delta, \mathbf{z}_c|\phi^*)$, where the “*” in θ^* and ϕ^* means that the parameter is not trained by the following calculated loss function. For details,

$$\begin{aligned} \mathbf{x}^+ &= \text{Gen}(\delta, \mathbf{z}_c|\phi) \\ &= \left\{ \tilde{\mathbf{x}}^0 \mid \tilde{\mathbf{x}}^{t-1} = \frac{1}{\sqrt{\alpha_t}} \left(\tilde{\mathbf{x}}^t - \frac{1 - \alpha_t}{\sqrt{1 - \alpha_t}} g_\phi(\tilde{\mathbf{x}}^t, t, \mathbf{z}_c^*) \right) + \sigma_t \mathcal{N}(0, 1), t \in \{T, \dots, 1\} \right\}, \end{aligned}$$

where T is the time step of the generation process, the initialized random noise $\tilde{\mathbf{x}}^T = \delta$. The $g_\phi(\cdot)$ is a neural network approximator intended to predict δ with $\tilde{\mathbf{x}}$ and the condition vector \mathbf{z}_c^* . The random noise vector $\delta \sim \mathcal{N}(0, \mathbf{1})$ is the initialized data, and \mathbf{z}_c is a conditional vector with $\mathbf{z}_c = \text{Enc}(\mathbf{x}_c|\theta^*)$. The α_t is the noise parameter in the diffusion process, and $\bar{\alpha}_t = 1 - \alpha_t$. The \mathbf{z}_c is trained by the loss function of Eq. (5). At the beginning of the training, in order to avoid unstable positive samples from the freshly initialized generative model, the augmented data are come from model-free approaches.

After obtaining the background set \mathcal{X} , the data is mapped to the semantic latent space $\mathcal{Y} = \{\mathbf{y}_c, \mathbf{y}_1, \dots, \mathbf{y}_j, \dots, \mathbf{y}_B\}$, $\mathcal{Z} = \{\mathbf{z}_c, \mathbf{z}_1, \dots, \mathbf{z}_j, \dots, \mathbf{z}_B\}$ through the semantic encoder $\mathbf{y}_j, \mathbf{z}_j = \text{Enc}(\mathbf{x}_j|\theta)$. The soft contrastive learning loss is used to train the semantic encoder,

$$\mathcal{L}_{\text{scl}}(\mathcal{Y}, \mathcal{Z}) = -\sum_{j=1}^B \{P(\mathbf{y}_c, \mathbf{y}_j) \log(Q(\mathbf{z}_c, \mathbf{z}_j)) + (1 - P(\mathbf{y}_c, \mathbf{y}_j)) \log(1 - Q(\mathbf{z}_c, \mathbf{z}_j))\}, \quad (2)$$

where the $P(\mathbf{a}, \mathbf{b})$ is soft learning weight, and $Q(\mathbf{a}, \mathbf{b})$ is density ratio,

$$P(\mathbf{a}, \mathbf{b}) = (1 + \mathcal{H}_{ij}(e^\beta - 1)) \mathcal{S}(\mathbf{a}, \mathbf{b}), \quad Q(\mathbf{a}, \mathbf{b}) = \mathcal{S}(\mathbf{a}, \mathbf{b}). \quad (3)$$

where hyper-parameter $\beta \in [0, 1]$ introduces prior knowledge of data augmentation relationship \mathcal{H}_{ij} into the model training. To map the high-dimensional embedding vector to a probability value, a kernel function $\mathcal{S}(\cdot)$ is used. In this paper, we use the t-distribution kernel function $\mathcal{S}^\nu(\cdot)$ because it exposes the degrees of freedom and allows us to adjust the closeness of the distribution in the dimensionality reduction mapping (Li et al., 2021a). The t-distribution kernel function is defined as follows,

$$\mathcal{S}(\mathbf{z}_i, \mathbf{z}_j) = \Gamma((\nu + 1)/2) (1 + \|\mathbf{z}_i - \mathbf{z}_j\|_2^2/\nu)^{-\frac{\nu+1}{2}} / \sqrt{\nu\pi}\Gamma(\nu/2) \quad (4)$$

where $\Gamma(\cdot)$ is the Gamma function. The degrees of freedom ν control the shape of the kernel function. The different degrees of freedom (ν^y, ν^z) is used in \mathcal{R}^y and \mathcal{R}^z for the dimensional reduction mapping.

To avoid getting unstable augmented data from the randomly initialized generator, we used a traditional hand-designed data augmentation tool to launch the semantic encoder. Specifically, training starts exclusively with the traditional data augmentation tool and is replaced with DiffAug-generated data substitutions after startup, with the probability of substitution being the hyperparameter α .

In the generative modeling step, diffusion generator $\text{Gen}(\cdot)$ is trained by the vanilla diffusion loss $\mathcal{L}_{\text{df}}(\mathbf{x}_c, \mathbf{z}_c|\phi)$ (Ho et al., 2020),

$$L_{\text{df}}(\mathbf{x}_c, \mathbf{z}_c|\phi) = \sum_{t=1}^T \left\{ \left\| \delta - g_\phi(\sqrt{\bar{\alpha}_t}\tilde{\mathbf{x}}_c^t + \sqrt{1 - \bar{\alpha}_t}, t, \mathbf{z}_c) \right\|_2^2 \right\}, \quad (5)$$

where, the conditional vector \mathbf{z}_c is generated from the semantic encoder. The $g_\phi(\cdot)$ is the conditional diffusion neural network.

The overall loss function of DiffAug is defined as follows,

$$\mathcal{L} = \mathcal{L}_{\text{scl}}(\mathcal{Y}, \mathcal{Z}) + L_{\text{df}}(\mathbf{x}_c, \mathbf{z}_c|\phi), \quad (6)$$

For inference, given the trained semantic encoder $\text{Enc}(\cdot|\theta)$ and diffusion generator $D(\cdot)$, and DiffAug generate new augmented data \mathbf{x}_i^+ from any input data \mathbf{x}_i .

$$\mathbf{x}_i^+ = \text{Gen}(\delta|\mathbf{z}_i), \quad \mathbf{y}_i, \mathbf{z}_i = \text{Enc}(\mathbf{x}_i), \quad (7)$$

Meanwhile, DiffAug’s semantic encoder can be seen as a feature extractor. It is considered to have good discriminative performance because it is trained at the same time as the diffusion generator. The algorithm for generating the new data is shown in Algorithm 1.

4 RESULTS

We evaluate the effectiveness of the proposed DiffAug on (classification/linear test, clustering, visualization) and analyze each proposed component. We also compare DiffAug with the SOTA methods on the Biological and CV datasets. The results show that DiffAug can generate meaningful augmentation data which can improve the contrastive learning. The detailed experimental settings are in Appendix.

Algorithm 1 The DiffAug Augmented Data Generating Algorithm:

Input: Data: $\mathcal{D}_t = \{\mathbf{x}_c\}_{i=1}^N$, Learning rate: η , Epochs: E , Batch size: B , α , Network: $\text{Enc}_\theta, \text{Gen}_\phi$,**Output:** New augmented data: $\{x^+\}_{i=1}^N$ for any data $\{x\}_{i=1}^N$.

```
1: while  $i = 0; i < E; i++$  do
2:    $\phi, \theta \leftarrow \text{Init}()$ . # Init the network parameters
3:   while  $b = 0; b < \lceil |\mathcal{X}|/B \rceil; b++$  do
4:      $\mathbf{x}_c \sim \mathcal{D}_t$ ; # Sample the centering data.
5:      $\mathbf{y}_c, \mathbf{z}_c \leftarrow \text{Enc}(\mathbf{x}_c|\theta)$ ; # Generate frozen condition vector.
6:      $L_1 \leftarrow L_{\text{df}}(\mathbf{x}_c, \text{SG}(\mathbf{z}_c)|\phi)$  by Eq. (5); # Cal. diffusion loss
7:      $\mathcal{X} = \{\mathbf{x}_c, \mathbf{x}_1, \dots, \mathbf{x}_B | \mathbf{x}_j \sim \mathcal{D}_t \text{ if } \mathcal{H}_{ij} = 0; \mathbf{x}_j \sim \text{Aug}(\mathbf{x}_c) \text{ else}\}$ ; # Generate/sample data
8:      $\mathcal{Y} = \{\mathbf{y}_c, \mathbf{y}_1, \dots, \mathbf{y}_j, \dots, \mathbf{y}_B\}$ ,  $\mathcal{Z} = \{\mathbf{z}_c, \mathbf{z}_1, \dots, \mathbf{z}_j, \dots, \mathbf{z}_B\}$ ,  $\mathbf{y}_j, \mathbf{z}_j = \text{Enc}(\mathbf{x}_j|\theta)$ 
9:      $L_2 \leftarrow L_{\text{scl}}(\mathcal{Y}, \mathcal{Z})$  by Eq. (2); # Cal. scl loss
10:     $\phi \leftarrow \phi - \eta \frac{\partial L_1}{\partial \phi}$ ,  $\theta \leftarrow \theta - \eta \frac{\partial L_2}{\partial \theta}$ ; # Update parameters
11:  end while
12: end while
13:  $\{\mathbf{x}_c^+ \leftarrow \text{Gen}(\mathbf{z}_c|\phi), \mathbf{y}_c, \mathbf{z}_c \leftarrow \text{Enc}(\mathbf{x}_c|\theta)\}_{i=1}^N$ ; # Generate. the new embedding results
```

4.1 COMPARISON ON BIOLOGICAL DATASET

In this section, we compare DiffAug with state-of-the-art (SOTA) methods on biological datasets. Furthermore, we explore whether DiffAug can surpass manual design augmentation approaches. The comparative results using linear SVM performance and kMeans clustering performance are provided in Table 2.

Baseline methods and datasets The methods chosen for comparison encompass both parameter-free dimensional reduction techniques (Wang et al., 2021) and parameter-based methods. The latter category includes ivis (Szubert et al., 2019), PHATE (Moon & van Dijk, 2019), parametric UMAP (McInnes et al., 2018; Sainburg et al., 2021), and DMTEV (Zang et al., 2022a). Experiments are performed on six biological datasets: HCL, Gast, SAM, MCA, and two others not specified.

Test protocols To assess the efficacy of the proposed methods, we utilized both linear SVM performance and kMeans clustering. For the linear SVM evaluation, embeddings were partitioned with 90% designated for training and 10% for testing; the training set facilitated the linear SVM training, while the test set yielded the performance metrics. In the kMeans clustering evaluation, the procedure was analogous but employed kMeans in lieu of the linear SVM, mirroring the setup described in DMTEV. Detailed specifics of this configuration are elaborated in the Appendix. To ensure consistent comparisons across all methodologies, input data was projected into a 2D space, and evaluations were executed using 10-fold cross-validation. Comprehensive insights regarding datasets, baseline methods, and evaluation metrics are also available in the Appendix.

Model settings For DiffAug, both the semantic encoder $\text{Enc}(\cdot)$, and the diffusion generator $\text{Gen}(\cdot)$, are implemented using a Multi-Layer Perceptron (MLP). Their respective architectures are defined as: $\text{Enc}(\cdot)$: [-1, 500, 300, 80], $\text{Gen}(\cdot)$: [-1, 500, 80, 500, -1]. Here, the value -1 stands for the dimension of the input data.

Analysis As illustrated in Table 2, DiffAug outperforms all other techniques in eight practical evaluations spanning four datasets, achieving a performance boost ranging from 1.1% to 11.1% over its competitors. We discerned several distinct advantages of DiffAug, particularly in classification and clustering metrics: (a) DiffAug’s data augmentation improves performance more than compared methods. This improvement is likely because these methods don’t have effective data augmentation techniques. Properly augmenting biological data can lead to better results. (b) Data processed by DiffAug has less overlap between different groups, which helps in better classification and clustering. This might be because DiffAug creates clearer boundaries between different data categories, leading to more accurate test results. (c) DiffAug’s approach can be added to other unsupervised learning methods. Until now, it’s been challenging to find effective data augmentation techniques in biology. We believe DiffAug offers new opportunities in this field.

Table 2: **Comparison of the Linear-test and KMeans clustering performance on biological dataset.** The best results are marked in **bold**. The improvement over the best baseline is shown in parentheses. Boosts over 2.5% are shown by underline. The ‘AVE’ represents the mean of the performance on the four datasets.

	Linear-test Performance					KMeans Clustering Performance				
	HCL	Gast	SAM	MCA	AVE	HCL	Gast	SAM	MCA	AVE
PUMAP	63.6	66.5	59.9	62.2	63.1	67.8	60.3	40.3	55.7	56.0
Ivis	24.4	45.6	45.6	45.8	40.4	59.8	36.0	31.9	56.3	46.0
PHATE	53.8	71.5	71.5	61.3	64.5	45.6	61.9	62.5	66.8	59.2
PaCMAP	66.2	83.7	83.7	61.3	73.7	73.7	71.2	66.5	70.9	70.6
DMTEV	68.3	84.6	83.6	64.2	75.2	74.1	71.4	66.7	71.1	70.8
DiffAug	<u>72.7</u> ^(+4.4)	<u>91.8</u> ^(+6.2)	<u>74.7</u> ^(+11.1)	<u>67.4</u> ^(+3.2)	<u>79.1</u> ^(+3.9)	<u>77.0</u> ^(+2.9)	<u>72.5</u> ^(+1.1)	<u>70.6</u> ^(+3.9)	<u>74.1</u> ^(+3.0)	<u>73.6</u> ^(+2.8)

Table 3: **Comparison of Linear-test and KMeans clustering performance on computer vision dataset.** BYOL⁺ and SimSiam⁺ are the results of BYOL and SimSiam with DiffAug’s augmentation results. Improvements over the best baseline are shown in parentheses. Best results are marked in **bold**. The improvement over the best baseline is shown in parentheses. Boosts over 2.0% are shown by underline. The ‘AVE’ represents the mean of the performance on the four datasets.

	Linear-test Performance					KMeans Clustering Performance				
	CF10	CF100	STL10	TINet	AVE	CF10	CF100	STL10	TINet	AVE
SimCLR	84.2	48.5	86.9	38.4	64.5	64.4	38.6	77.2	12.9	48.2
MoCoV2	85.2	56.3	85.6	39.4	66.6	65.9	36.4	75.4	14.4	48.0
MAE (LT)	72.5	32.6	78.4	—	—	68.3	42.6	84.1	—	—
DLME	91.3	66.1	90.1	44.9	73.1	82.2	44.1	88.3	18.2	58.2
BYOL	82.4	57.4	88.7	43.8	68.0	62.6	45.6	78.5	18.8	51.3
SimSiam	83.1	56.7	84.8	44.9	67.3	79.3	42.1	82.8	18.9	55.7
BYOL ⁺	<u>83.1</u> ^(+0.7)	<u>59.4</u> ^(+2.0)	<u>89.8</u> ^(+1.1)	<u>45.6</u> ^(+1.8)	<u>69.4</u> ^(+1.4)	<u>65.7</u> ^(+3.1)	<u>45.6</u> ^(+0.0)	<u>80.1</u> ^(+1.6)	<u>20.7</u> ^(+1.9)	<u>53.0</u> ^(+1.7)
SimSiam ⁺	<u>87.3</u> ^(+4.2)	<u>60.1</u> ^(+3.4)	<u>88.5</u> ^(+3.7)	<u>45.3</u> ^(+0.4)	<u>70.3</u> ^(+3.0)	<u>80.1</u> ^(+0.8)	<u>46.9</u> ^(+4.8)	<u>83.6</u> ^(+0.8)	<u>19.9</u> ^(+1.0)	<u>60.1</u> ^(+4.6)
DiffAug	<u>93.4</u> ^(+2.1)	<u>69.9</u> ^(+3.8)	<u>92.5</u> ^(+2.4)	<u>49.7</u> ^(+5.2)	<u>75.8</u> ^(+2.7)	<u>86.2</u> ^(+6.0)	<u>48.6</u> ^(+3.0)	<u>89.4</u> ^(+2.1)	<u>19.8</u> ^(+1.6)	<u>60.6</u> ^(+2.4)

4.2 COMPARISON ON VISION DATASET

Next, we demonstrate that DiffAug can be used for data from a variety of domains while arguing that DiffAug can bring enhancements in data from vision. Specifically, we compare DiffAug with SOTA methods on vision datasets. Furthermore, we explore whether DiffAug can surpass manual design augmentation approaches. The comparative results using linear-test performance and kMeans clustering performance are provided in Table 3.

Baseline methods and datasets The methods chosen for comparison encompass famous contrastive learning methods, including SimCLR (Chen et al., 2020), MOCO v2 (He et al., 2020), BYOL (Grill et al., 2020), SimSiam (Chen & He, 2021) and DLME (Zang et al., 2022b). Experiments are performed on four vision datasets: CIFAR-10 [CF10] and CIFAR-100 [CF100] (Krizhevsky et al., 2009), STL10 (Coates et al., 2011), TinyImageNet [TINet] (Le & Yang, 2015).

Test protocols In the Linear-test performance assessment, akin to SimCLR (Chen et al., 2020), we linearly evaluated the model’s representations atop the frozen features, ensuring the quality of the learned representations was solely due to the pre-training task, devoid of any subsequent fine-tuning influence. The ResNet50 (He et al., 2015) backbone from the baseline was directly employed, while for comparison, the DiffAug semantic encoder was utilized, acting as the contrast learning backbone trained with augmented images from DiffAug. For the kMeans clustering evaluation, feature vectors from the models were extracted, excluding the top classification layer, and kMeans clustering was subsequently applied to these features, with clustering accuracy serving as the primary evaluation metric.

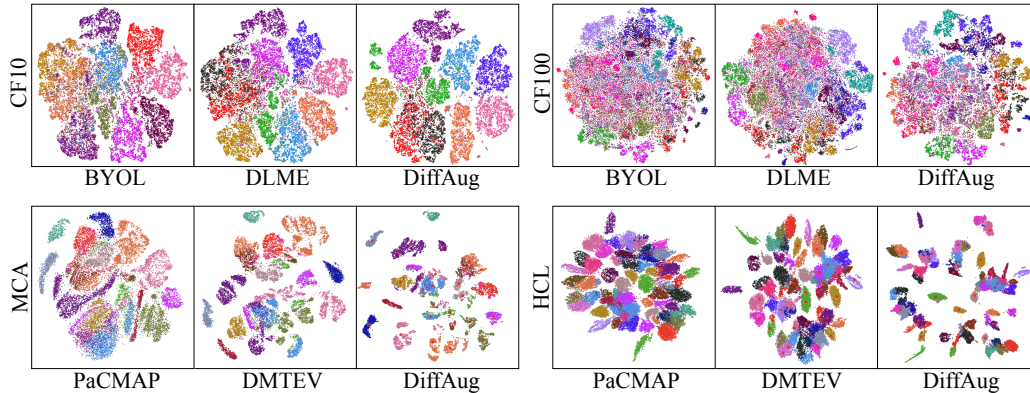


Figure 3: **Visualization Analyse.** t-SNE (Van der Maaten & Hinton, 2008) visualization results of the latent space of BYOL, DLME, and DiffAug on CF10, CF100, MCA and HCL dataset. The top three methods of performance performance were included.

Analysis As depicted in Table 3, DiffAug consistently eclipses state-of-the-art (SOTA) methods across all datasets, outshining other techniques by a minimum of 2% in six of the eight projects and boosting average metrics by at least 2.4% over the evaluated methods. This performance accentuates DiffAug’s superior data augmentation prowess. (a) Notably, DiffAug’s advantages aren’t confined to biological data but also extend to areas like computer vision, where data augmentation strategies are typically more straightforward. (b) This versatility suggests that DiffAug’s approach rivals, if not exceeds, conventional hand-crafted methods. Furthermore, the encoder in DiffAug yields robust discriminative features, and by leveraging its data augmentation—which expands the dataset by a factor of five—the performance of the base method sees a substantial uplift. (c) However, for datasets with a multitude of classes, such as CF100 and TinyImageNet, DiffAug’s encoder might not always capture clustering nuances perfectly. Yet, the augmented data remains instrumental, guiding comparative learning to achieve enhanced discriminative outcomes.

4.3 LATENT SPACE VISUALIZATION AND FURTHERMORE ANALYSIS

Next, in order to explore and confirm the enhancements obtained by DiffAug in different domains, we will visualize the latent space containing DiffAug and the baseline method. The visualization results are shown in Fig. 3.

Experimental setups We selected the CF10, CF100, MCA, and HCL datasets for our visualization exercise. The choice of these datasets stems from their inherent diversity, which offers an exhaustive assessment of the latent space quality spanning various data types and structures. For visualization, we incorporated models namely BYOL, DLME, and DiffAug. According to our assessments, these models emerge as the top three in terms of performance. This ensures our analysis is centered around contrasting the crème de la crème of architectures. The parameters chosen for t-SNE visualization comprised a perplexity of 30 coupled with a learning rate of 200. Such parameters were zeroed in upon post multiple test runs, guaranteeing optimal delineation and portrayal of data clusters. The setup and dataset used for the experiments are the same as in Sec. 4.1 and Sec. 4.2.

Analysis From the visualization results in Fig. 3, we deduce that DiffAug exhibits exceptional discriminative capabilities across all datasets, which is pivotal to its performance enhancement. Notably, image data representations appear denser than those from biological data, suggesting a tighter similarity in their latent spaces. Moreover, DiffAug’s representations of biological data are distinctly more clustered, elucidating its notable performance boost, especially on biological datasets.

4.4 ABLATION STUDY

Ablation study of the semantic encoder. For Ablation in Table. 4, the ‘(A1) Gen($\cdot|\phi$) + Supervised Condition’ directly utilizes supervised conditionals, sidestepping condition vectors produced

Table 4: **Ablation study of the semantic encoder includes DiffAug’s encoder is necessary and can efficiently generate conditional vectors.** Linear-tests performance of different ablation setups on on vision dataset and biological dataset.

Datasets	Vision Datasets				Biological Datasets			
	CF10	CF100	STL10	TINet	HCL	Gast	Sam	MCA
(A1) Gen($\cdot \phi$) + Supervised Condition	93.4	70.9	92.9	45.9	72.9	92.1	74.6	70.1
(A2) Gen($\cdot \phi$) + Random Condition	34.2	10.4	30.1	7.3	18.2	5.6	6.9	13.1
(A3) Gen($\cdot \phi$)+Enc($\cdot \theta$) (DiffAug)	93.4	69.9	92.5	49.7	72.7	91.8	74.7	67.4

Table 5: **Ablation study of training strategy and scl loss function includes current training strategy is effective and the scl loss can lead to a boost.** Linear-tests performance of different ablation setups on on vision dataset and biological dataset.

Datasets	Vision Datasets				Biological Datasets			
	CF10	CF100	STL10	TINet	HCL	Gast	Sam	MCA
(B1) SimCLR	91.3	66.1	90.1	44.9	68.3	85.6	63.6	58.3
(B2) DiffAug w/o $L_{df}(x_c, z_c \phi)$	91.3	66.1	90.1	44.9	68.3	85.6	63.6	58.3
(B3) DiffAug w/o $\mathcal{L}_{scl}(\mathcal{Y}, \mathcal{Z})$	92.7	68.4	90.9	45.1	71.6	86.9	67.3	58.7
(B4) DiffAug + EM training	92.9	69.7	92.7	45.3	72.7	91.7	74.6	60.1
(B5) $\mathcal{L}_{scl}(\mathcal{Y}, \mathcal{Z}) + L_{df}(x_c, z_c \phi)$ (DiffAug)	93.4	69.9	92.5	49.7	72.7	91.8	74.7	67.4

by the unsupervised neural network. The ‘(A2) Gen($\cdot|\phi$) + Random Condition’ adopts randomized conditional vectors in lieu of encoder-generated ones. ‘(A3) Gen($\cdot|\phi$)+Enc($\cdot|\theta$) (DiffAug)’ pertains the proposed DiffAug method. From Table 4, the robustness and innovation of DiffAug’s design become evident. (a) The outcomes of (A1), (A2), and (A3) highlight the significance of semantic encoders. Replacing their output with randomized conditions leads to erratic training results. Interestingly, DiffAug’s output mirrors the fully supervised condition, indicating its capability to mimic supervised labeling in an unsupervised context.

Ablation study of training strategy and scl loss function. For Ablation in Table. 5, ‘(B1) SimCLR’ means that the model is trained by SimCLR (Chen et al., 2020). ‘(B2) DiffAug w/o $L_{df}(x_c, z_c|\phi)$ ’ omits the diffusion loss and train the encoder with only the soft contrastive learning loss. ‘(B3) DiffAug w/o $\mathcal{L}_{scl}(\mathcal{Y}, \mathcal{Z})$ ’ omits the soft contrastive learning loss and train the encoder with InfoNCE loss. ‘(B4) DiffAug + EM training’ and ‘(B5) $\mathcal{L}_{scl}(\mathcal{Y}, \mathcal{Z}) + L_{df}(x_c, z_c|\phi)$ (DiffAug)’ talk about the training strategy of DiffAug. The B4 means training the model by alternating between the two loss functions. The B5 means training the model by integrating the two loss functions. The results from these experiments can be found in Table 5. From (B1), (B2), (B4), and (B5) accentuate the importance of the soft contrastive learning (scl) loss. From (B4), and (B5) accentuate both integrated and separate learning strategies yield similar results, but the integrated method stands out for its efficiency, making it our method of choice.

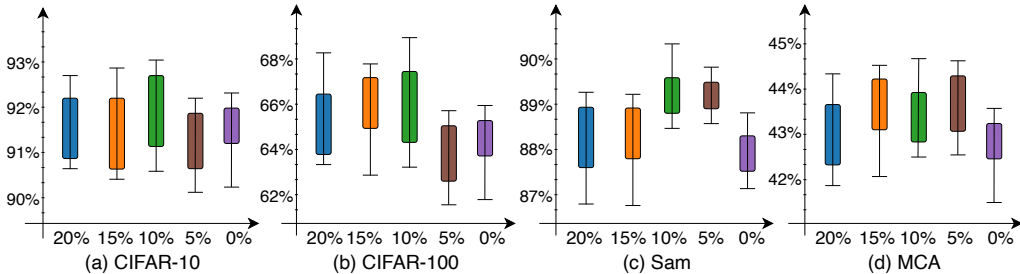


Figure 4: **Hypter-parametric analysis.** The Box plots of augmentation strength hyperparameters α and model Linear-tests performance. For each parameter, statistical results of experiments based on grid search were performed.

4.5 HYPTER-PARAMETRIC ANALYSIS

We delved into the performance enhancements and potential toxicity of the DiffAug method through hyperparametric analysis. The hyperparameter α dictates the influence of DiffAug’s results on the semantic coder’s training. Introducing minimal augmented data reverts the method to a traditional approach, while an excess can lead to encoder toxicity.

Experimental Setups We used grid search on two vision datasets (CF10, CF100) and two biological datasets (SAM and MCA) to explore the effect on performance of the proportion of use data augmentation controlled by α . The experimental framework and datasets are the same as in Sec. 4.1 and Sec. 4.2.

Analysis As the results shown in Fig. 4, the relative performance of alpha values remains consistently stable across experiments on different datasets. That is, alpha values of 10%-15% seem to be optimal for the tested datasets. We consider that $\alpha = 10\%$ may be an appropriate default setting.

5 CONCLUSION

In conclusion, we have introduced a novel and efficient data augmentation framework, DiffAug, that utilizes diffusion-based augmentation and deep clustering to improve the robustness and generalization of self-supervised contrastive learning methods. DiffAug does not rely on prior knowledge or externally labeled data, making it a universal augmentation framework that demonstrates impressive performance in both vision and life science data domains. Our experiments show that DiffAug consistently improves classification and clustering accuracy on various datasets, including CF10, CF100, STL10, Tiny-ImageNet, HCL, Gast, Sam, MCA, and MAU. We believe that DiffAug has the potential to become a standard data augmentation technique in the field of self-supervised learning. The code for DiffAug is publicly available, and we encourage researchers to explore its potential for their own applications.

REFERENCES

- Antreas Antoniou, Amos Storkey, and Harrison Edwards. Data augmentation generative adversarial networks, 2017. URL <https://arxiv.org/abs/1711.04340>.
- Mahmoud Assran, Mathilde Caron, Ishan Misra, Piotr Bojanowski, Florian Bordes, Pascal Vincent, Armand Joulin, Mike Rabbat, and Nicolas Ballas. Masked siamese networks for label-efficient learning. In *ECCV*, pp. 456–473. Springer, 2022.
- Victor Besnier, Himalaya Jain, Andrei Bursuc, Matthieu Cord, and Patrick Pérez. This dataset does not exist: Training models from generated images. In *ICASSP 2020*, pp. 1–5. IEEE, 2020. doi: 10.1109/ICASSP40776.2020.9053146. URL <https://doi.org/10.1109/ICASSP40776.2020.9053146>.
- Alexandre Blanco-Gonzalez, Alfonso Cabezon, Alejandro Seco-Gonzalez, Daniel Conde-Torres, Paula Antelo-Riveiro, Angel Pineiro, and Rebeca Garcia-Fandino. The role of ai in drug discovery: challenges, opportunities, and strategies. *Pharmaceuticals*, 16(6):891, 2023.
- Andrea Botton, Gianmarco Barberi, and Pierantonio Facco. Data augmentation to support biopharmaceutical process development through digital models—a proof of concept. *Processes*, 10(9):1796, 2022.
- Andrew Brock, Jeff Donahue, and Karen Simonyan. Large scale GAN training for high fidelity natural image synthesis. In *ICLR 2019*, 2019. URL <https://openreview.net/forum?id=B1xsqj09Fm>.
- Clément Chadebec, Elina Thibeau-Sutre, Ninon Burgos, and Stéphanie Allassonnière. Data augmentation in high dimensional low sample size setting using a geometry-based variational autoencoder. *PAMI*, 45(3):2879–2896, 2022.
- Ting Chen, Simon Kornblith, Mohammad Norouzi, and Geoffrey Hinton. A Simple Framework for Contrastive Learning of Visual Representations. *arXiv:2002.05709 [cs, stat]*, June 2020. URL <http://arxiv.org/abs/2002.05709>. arXiv: 2002.05709.
- Xinlei Chen and Kaiming He. Exploring simple siamese representation learning. In *CVPR*, pp. 15750–15758, 2021.
- Adam Coates, Andrew Ng, and Honglak Lee. An analysis of single-layer networks in unsupervised feature learning. In *Proceedings of the fourteenth international conference on artificial intelligence and statistics*, pp. 215–223. JMLR Workshop and Conference Proceedings, 2011.
- Ekin D Cubuk, Barret Zoph, Dandelion Mane, Vijay Vasudevan, and Quoc V Le. Autoaugment: Learning augmentation strategies from data. In *CVPR*, pp. 113–123, 2019.
- Ekin D Cubuk, Barret Zoph, Jonathon Shlens, and Quoc V Le. Randaugment: Practical automated data augmentation with a reduced search space. In *CVPR*, pp. 702–703, 2020.
- Jiequan Cui, Zhisheng Zhong, Shu Liu, Bei Yu, and Jiaya Jia. Parametric contrastive learning. In *ICCV*, pp. 715–724, 2021.
- Pham Thanh Dat, Anuvabh Dutt, Denis Pellerin, and Georges Quénot. Classifier training from a generative model. In *2019 International Conference on Content-Based Multimedia Indexing (CBMI)*, pp. 1–6, 2019. doi: 10.1109/CBMI.2019.8877479.
- Prafulla Dhariwal and Alexander Quinn Nichol. Diffusion models beat gans on image synthesis. In Marc’Aurelio Ranzato, Alina Beygelzimer, Yann N. Dauphin, Percy Liang, and Jennifer Wortman Vaughan (eds.), *NeurIPS 2021*, pp. 8780–8794, 2021. URL <https://proceedings.neurips.cc/paper/2021/hash/49ad23d1ec9fa4bd8d77d02681df5cfa-Abstract.html>.
- Ian Goodfellow, Jean Pouget-Abadie, Mehdi Mirza, Bing Xu, David Warde-Farley, Sherjil Ozair, Aaron Courville, and Yoshua Bengio. Generative adversarial nets. In Z. Ghahramani, M. Welling, C. Cortes, N. Lawrence, and K.Q. Weinberger (eds.), *NeurIPS*, volume 27. Curran Associates, Inc., 2014. URL <https://proceedings.neurips.cc/paper/2014/file/5ca3e9b122f61f8f06494c97b1afccf3-Paper.pdf>.

-
- Jean-Bastien Grill, Florian Strub, Florent Alché, Corentin Tallec, Pierre H. Richemond, Elena Buchatskaya, Carl Doersch, Bernardo Avila Pires, Zhaohan Daniel Guo, Mohammad Gheshlaghi Azar, Bilal Piot, Koray Kavukcuoglu, Rémi Munos, and Michal Valko. Bootstrap Your Own Latent: A New Approach to Self-Supervised Learning. *arXiv:2006.07733 [cs, stat]*, June 2020. URL <http://arxiv.org/abs/2006.07733>. arXiv: 2006.07733.
- Xi Han, Liheng Zhang, Kang Zhou, and Xiaonan Wang. Progan: Protein solubility generative adversarial nets for data augmentation in dnn framework. *Computers & Chemical Engineering*, 131:106533, 2019.
- Ayaan Haque. EC-GAN: low-sample classification using semi-supervised algorithms and gans (student abstract). In *AAAI*, pp. 15797–15798, 2021. URL <https://ojs.aaai.org/index.php/AAAI/article/view/17895>.
- Kaiming He, Xiangyu Zhang, Shaoqing Ren, and Jian Sun. Deep Residual Learning for Image Recognition. *arXiv:1512.03385 [cs]*, December 2015. URL <http://arxiv.org/abs/1512.03385>. arXiv: 1512.03385.
- Kaiming He, Haoqi Fan, Yuxin Wu, Saining Xie, and Ross Girshick. Momentum Contrast for Unsupervised Visual Representation Learning. *arXiv:1911.05722 [cs]*, March 2020. URL <http://arxiv.org/abs/1911.05722>. arXiv: 1911.05722.
- Kaiming He, Xinlei Chen, Saining Xie, Yanghao Li, Piotr Dollár, and Ross Girshick. Masked autoencoders are scalable vision learners. 2021.
- Ruifei He, Shuyang Sun, Xin Yu, Chuhui Xue, Wenqing Zhang, Philip Torr, Song Bai, and Xiaojuan Qi. Is synthetic data from generative models ready for image recognition?, 2022. URL <https://arxiv.org/abs/2210.07574>.
- Jonathan Ho and Tim Salimans. Classifier-free diffusion guidance, 2022. URL <https://arxiv.org/abs/2207.12598>.
- Jonathan Ho, Ajay Jain, and Pieter Abbeel. Denoising diffusion probabilistic models. In Hugo Larochelle, Marc’Aurelio Ranzato, Raia Hadsell, Maria-Florina Balcan, and Hsuan-Tien Lin (eds.), *NeurIPS*, 2020. URL <https://proceedings.neurips.cc/paper/2020/hash/4c5bcfec8584af0d967f1ab10179ca4b-Abstract.html>.
- Hai-Hui Huang, Hao Rao, Rui Miao, and Yong Liang. A novel meta-analysis based on data augmentation and elastic data shared lasso regularization for gene expression. *BMC bioinformatics*, 23(Suppl 10):353, 2022.
- Sheng-Wei Huang, Che-Tsung Lin, Shu-Ping Chen, Yen-Yi Wu, Po-Hao Hsu, and Shang-Hong Lai. Auggan: Cross domain adaptation with gan-based data augmentation. In *ECCV*, pp. 718–731, 2018.
- Ali Jahanian, Xavier Puig, Yonglong Tian, and Phillip Isola. Generative models as a data source for multiview representation learning. In *ICLR*, 2022. URL <https://openreview.net/forum?id=qhAeZjs7dCL>.
- Nour Eldeen Khalifa, Mohamed Loey, and Seyedali Mirjalili. A comprehensive survey of recent trends in deep learning for digital images augmentation. *Artificial Intelligence Review*, pp. 1–27, 2022.
- Diederik P. Kingma and Max Welling. Auto-encoding variational bayes. In Yoshua Bengio and Yann LeCun (eds.), *ICLR*, 2014. URL <http://arxiv.org/abs/1312.6114>.
- Rayan Krishnan, Pranav Rajpurkar, and Eric J Topol. Self-supervised learning in medicine and healthcare. *Nature Biomedical Engineering*, pp. 1–7, 2022.
- Alex Krizhevsky, Geoffrey Hinton, et al. Learning multiple layers of features from tiny images. 2009.
- Ya Le and Xuan Yang. Tiny imagenet visual recognition challenge. *CS 231N*, 7(7):3, 2015.

-
- Bolian Li, Zongbo Han, Haining Li, Huazhu Fu, and Changqing Zhang. Trustworthy long-tailed classification. *arXiv: Learning*, 2021a.
- Menglu Li and Wen Zhang. Phiaf: prediction of phage-host interactions with gan-based data augmentation and sequence-based feature fusion. *Briefings in Bioinformatics*, 23(1):bbab348, 2022.
- Pu Li, Xiaobai Liu, and Xiaohui Xie. Learning sample-specific policies for sequential image augmentation. In *Proceedings of the 29th ACM International Conference on Multimedia*, MM '21, pp. 4491–4500, New York, NY, USA, 2021b. Association for Computing Machinery. ISBN 9781450386517. doi: 10.1145/3474085.3475602. URL <https://doi.org/10.1145/3474085.3475602>.
- Kiran Maharana, Surajit Mondal, and Bhushankumar Nemade. A review: Data pre-processing and data augmentation techniques. *Global Transitions Proceedings*, 3(1):91–99, 2022.
- Miles McGibbon, Sam Money-Kyrle, Vincent Blay, and Douglas R Houston. Scorch: improving structure-based virtual screening with machine learning classifiers, data augmentation, and uncertainty estimation. *Journal of Advanced Research*, 46:135–147, 2023.
- Leland McInnes, John Healy, and James Melville. UMAP: Uniform Manifold Approximation and Projection for Dimension Reduction. *arXiv:1802.03426 [cs, stat]*, February 2018. URL <http://arxiv.org/abs/1802.03426>. arXiv: 1802.03426 version: 1.
- Kevin R Moon and van Dijk. Visualizing structure and transitions in high dimensional biological data. *Nature biotechnology*, 37(12):1482–1492, 2019.
- Alexander Quinn Nichol and Prafulla Dhariwal. Improved denoising diffusion probabilistic models. In Marina Meila and Tong Zhang (eds.), *ICML*, volume 139 of *Proceedings of Machine Learning Research*, pp. 8162–8171. PMLR, 2021. URL <http://proceedings.mlr.press/v139/nichol21a.html>.
- Alexander Quinn Nichol, Prafulla Dhariwal, Aditya Ramesh, Pranav Shyam, Pamela Mishkin, Bob McGrew, Ilya Sutskever, and Mark Chen. GLIDE: towards photorealistic image generation and editing with text-guided diffusion models. In Kamalika Chaudhuri, Stefanie Jegelka, Le Song, Csaba Szepesvári, Gang Niu, and Sivan Sabato (eds.), *ICML*, volume 162 of *Proceedings of Machine Learning Research*, pp. 16784–16804. PMLR, 2022. URL <https://proceedings.mlr.press/v162/nichol22a.html>.
- Xiangyu Peng, Kai Wang, Zheng Zhu, Mang Wang, and Yang You. Crafting better contrastive views for siamese representation learning. In *CVPR 2022*, pp. 16031–16040, 2022.
- Aditya Ramesh, Prafulla Dhariwal, Alex Nichol, Casey Chu, and Mark Chen. Hierarchical text-conditional image generation with clip latents, 2022. URL <https://arxiv.org/abs/2204.06125>.
- Ali Razavi, Aäron van den Oord, and Oriol Vinyals. Generating diverse high-fidelity images with VQ-VAE-2. In Hanna M. Wallach, Hugo Larochelle, Alina Beygelzimer, Florence d’Alché-Buc, Emily B. Fox, and Roman Garnett (eds.), *NeurIPS 2019*, pp. 14837–14847, 2019. URL <https://proceedings.neurips.cc/paper/2019/hash/5f8e2fa1718d1bbcadf1cd9c7a54fb8c-Abstract.html>.
- Nils Rethmeier and Isabelle Augenstein. A primer on contrastive pretraining in language processing: Methods, lessons learned, and perspectives. *ACM Computing Surveys*, 55(10):1–17, 2023.
- Robin Rombach, Andreas Blattmann, Dominik Lorenz, Patrick Esser, and Björn Ommer. High-resolution image synthesis with latent diffusion models. In *CVPR 2022*, pp. 10674–10685. IEEE, 2022. doi: 10.1109/CVPR52688.2022.01042. URL <https://doi.org/10.1109/CVPR52688.2022.01042>.
- Chitwan Saharia, William Chan, Saurabh Saxena, Lala Li, Jay Whang, Emily Denton, Seyed Kamyar Seyed Ghasemipour, Burcu Karagol Ayan, S. Sara Mahdavi, Rapha Gontijo Lopes, Tim Salimans, Jonathan Ho, David J Fleet, and Mohammad Norouzi. Photorealistic text-to-image diffusion models with deep language understanding, 2022. URL <https://arxiv.org/abs/2205.11487>.

-
- Tim Sainburg, Leland McInnes, and Timothy Q. Gentner. Parametric UMAP embeddings for representation and semi-supervised learning. *arXiv:2009.12981 [cs, q-bio, stat]*, April 2021. URL <http://arxiv.org/abs/2009.12981>. arXiv: 2009.12981.
- Christoph Schuhmann, Romain Beaumont, Richard Vencu, Cade Gordon, Ross Wightman, Mehdi Cherti, Theo Coombes, Aarush Katta, Clayton Mullis, Mitchell Wortsman, Patrick Schramowski, Srivatsa Kundurthy, Katherine Crowson, Ludwig Schmidt, Robert Kaczmarczyk, and Jenia Jitsev. Laion-5b: An open large-scale dataset for training next generation image-text models, 2022. URL <https://arxiv.org/abs/2210.08402>.
- Yaoting Sun, Sathiyamoorthy Selvarajan, Zelin Zang, Wei Liu, Yi Zhu, Hao Zhang, Wanyuan Chen, Hao Chen, Lu Li, Xue Cai, et al. Artificial intelligence defines protein-based classification of thyroid nodules. *Cell discovery*, 8(1):85, 2022.
- Benjamin Szubert, Jennifer E. Cole, Claudia Monaco, and Ignat Drozdov. Structure-preserving visualisation of high dimensional single-cell datasets. *Scientific Reports*, 9(1):8914, June 2019. ISSN 2045-2322.
- Fabio Henrique Kiyoyi dos Santos Tanaka and Claus Aranha. Data augmentation using gans, 2019. URL <https://arxiv.org/abs/1904.09135>.
- Christina V Theodoris, Ling Xiao, Anant Chopra, Mark D Chaffin, Zeina R Al Sayed, Matthew C Hill, Helene Mantineo, Elizabeth M Brydon, Zexian Zeng, X Shirley Liu, et al. Transfer learning enables predictions in network biology. *Nature*, pp. 1–9, 2023.
- Yonglong Tian, Chen Sun, Ben Poole, Dilip Krishnan, Cordelia Schmid, and Phillip Isola. What makes for good views for contrastive learning? *NeurIPS*, 33:6827–6839, 2020.
- Toan Tran, Trung Pham, Gustavo Carneiro, Lyle J. Palmer, and Ian D. Reid. A bayesian data augmentation approach for learning deep models. In Isabelle Guyon, Ulrike von Luxburg, Samy Bengio, Hanna M. Wallach, Rob Fergus, S. V. N. Vishwanathan, and Roman Garnett (eds.), *NeurIPS 2017*, pp. 2797–2806, 2017. URL <https://proceedings.neurips.cc/paper/2017/hash/076023edc9187cflac1f1163470e479a-Abstract.html>.
- Laurens Van der Maaten and Geoffrey Hinton. Visualizing data using t-sne. *JMLR*, 9(11), 2008.
- Xiao Wang and Guo-Jun Qi. Contrastive learning with stronger augmentations. *TPAMI*, 45(5): 5549–5560, 2022.
- Yingfan Wang, Haiyang Huang, Cynthia Rudin, and Yaron Shaposhnik. Understanding how dimension reduction tools work: An empirical approach to deciphering t-sne, umap, trimap, and pacmap for data visualization. *JMLR*, 22(201):1–73, 2021. URL <http://jmlr.org/papers/v22/20-1061.html>.
- Sajila Wickramaratne and Md Shaad Mahmud. Conditional-gan based data augmentation for deep learning task classifier improvement using fnirs data. *Frontiers in Big Data*, 4:659146, 07 2021. doi: 10.3389/fdata.2021.659146.
- Wei Xiong, Yutong He, Yixuan Zhang, Wenhan Luo, Lin Ma, and Jiebo Luo. Fine-grained image-to-image transformation towards visual recognition. In *CVPR 2020*, June 2020.
- Mingle Xu, Sook Yoon, Alvaro Fuentes, and Dong Sun Park. A comprehensive survey of image augmentation techniques for deep learning. *Pattern Recognition*, pp. 109347, 2023.
- Shin’ya Yamaguchi, Sekitoshi Kanai, and Takeharu Eda. Effective data augmentation with multi-domain learning gans. In *AAAI 2020*, pp. 6566–6574. AAAI Press, 2020. URL <https://ojs.aaai.org/index.php/AAAI/article/view/6131>.
- Zipei Yan, Linchuan Xu, Atsushi Suzuki, Jing Wang, Jiannong Cao, and Jun Huang. Rgb color model aware computational color naming and its application to data augmentation. In *2022 IEEE International Conference on Big Data (Big Data)*, pp. 1172–1181. IEEE, 2022.
- Tianhao Yu, Haiyang Cui, Jianan Canal Li, Yunan Luo, Guangde Jiang, and Huimin Zhao. Enzyme function prediction using contrastive learning. *Science*, 379(6639):1358–1363, 2023.

-
- Zelin Zang, Shenghui Cheng, Linyan Lu, Hanchen Xia, Liangyu Li, Yaoting Sun, Yongjie Xu, Lei Shang, Baigui Sun, and Stan Z Li. Evnet: An explainable deep network for dimension reduction. *TVCG*, 2022a.
- Zelin Zang, Siyuan Li, Di Wu, Ge Wang, Kai Wang, Lei Shang, Baigui Sun, Hao Li, and Stan Z Li. Dlme: Deep local-flatness manifold embedding. *ECCV*, pp. 576–592, 2022b.
- Zelin Zang, Lei Shang, Senqiao Yang, Fei Wang, Baigui Sun, Xuansong Xie, and Stan Z. Li. Boosting novel category discovery over domains with soft contrastive learning and all-in-one classifier. 2023.
- Hongyi Zhang, Moustapha Cissé, Yann N. Dauphin, and David Lopez-Paz. mixup: Beyond empirical risk minimization. *CoRR*, abs/1710.09412, 2017. URL <http://arxiv.org/abs/1710.09412>.
- Junbo Zhang and Kaisheng Ma. Rethinking the augmentation module in contrastive learning: Learning hierarchical augmentation invariance with expanded views. In *CVPR 2022*, pp. 16650–16659, 2022.
- Yuhan Zhang, He Zhu, and Shan Yu. Adaptive data augmentation for contrastive learning. *ICASSP 2023*, pp. 1–5, 2023.
- Yuxuan Zhang, Wenzheng Chen, Huan Ling, Jun Gao, Yinan Zhang, Antonio Torralba, and Sanja Fidler. Image gans meet differentiable rendering for inverse graphics and interpretable 3d neural rendering. In *ICLR*. OpenReview.net, 2021a. URL <https://openreview.net/forum?id=yWkP7JuHX1>.
- Yuxuan Zhang, Huan Ling, Jun Gao, Kangxue Yin, Jean-Francois Lafleche, Adela Barriuso, Antonio Torralba, and Sanja Fidler. Datasetgan: Efficient labeled data factory with minimal human effort. In *CVPR*, pp. 10145–10155. Computer Vision Foundation / IEEE, 2021b. doi: 10.1109/CVPR46437.2021.01001. URL https://openaccess.thecvf.com/content/CVPR2021/html/Zhang_DatasetGAN_Efficient_Labeled_Data_Factory_With_Minimal_Human_Effort_CVPR_2021_paper.html.
- Zhedong Zheng, Liang Zheng, and Yi Yang. Unlabeled samples generated by GAN improve the person re-identification baseline in vitro. In *ICCV 2017*, pp. 3774–3782. IEEE Computer Society, 2017. doi: 10.1109/ICCV.2017.405. URL <https://doi.org/10.1109/ICCV.2017.405>.
- Zhiwei Zheng, Nguyen Quoc Khanh Le, and Matthew Chin Heng Chua. Maskdna-pgd: An innovative deep learning model for detecting dna methylation by integrating mask sequences and adversarial pgd training as a data augmentation method. *Chemometrics and Intelligent Laboratory Systems*, 232:104715, 2023.

A APPENDIX

You may include other additional sections here.